AIP | Applied Physics Letters

Effect of dislocation density on thermal boundary conductance across GaSb/GaAs interfaces

Patrick E. Hopkins, John C. Duda, Stephen P. Clark, Christopher P. Hains, Thomas J. Rotter et al.

Citation: Appl. Phys. Lett. **98**, 161913 (2011); doi: 10.1063/1.3581041
View online: http://dx.doi.org/10.1063/1.3581041
View Table of Contents: http://apl.aip.org/resource/1/APPLAB/v98/i16
Published by the American Institute of Physics.

Related Articles

Suppression of relaxation in (201) InGaN/GaN laser diodes using limited area epitaxy
Appl. Phys. Lett. 101, 241112 (2012)

The structure of dislocations in (In,Al,Ga)N wurtzite films grown epitaxially on (0001) or (112) GaN or AlN substrates
J. Appl. Phys. 112, 113507 (2012)

Analysis of critical dimensions for axial double heterostructure nanowires
J. Appl. Phys. 112, 114307 (2012)

Dislocation-induced fields in piezoelectric AlGaN/GaN bimaterial heterostructures
J. Appl. Phys. 112, 103501 (2012)

Indium incorporation efficiency and critical layer thickness of (201) InGaN layers on GaN
Appl. Phys. Lett. 101, 202102 (2012)

Additional information on Appl. Phys. Lett.

Journal Homepage: http://apl.aip.org/
Journal Information: http://apl.aip.org/about/about_the_journal
Top downloads: http://apl.aip.org/features/most_downloaded
Information for Authors: http://apl.aip.org/authors

ADVERTISEMENT

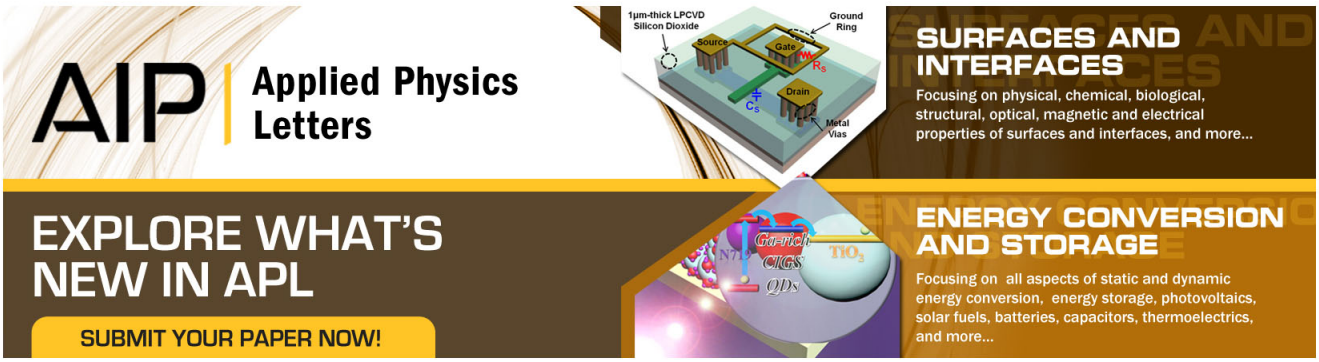

Effect of dislocation density on thermal boundary conductance across GaSb/GaAs interfaces

Patrick E. Hopkins,[1,2,a)] John C. Duda,[1,2] Stephen P. Clark,[3] Christopher P. Hains,[3] Thomas J. Rotter,[3] Leslie M. Phinney,[1] and Ganesh Balakrishnan[3]
[1]*Sandia National Laboratories, Albuquerque, New Mexico 87185, USA*
[2]*Department of Mechanical and Aerospace Engineering, University of Virginia, Charlottesville, Virginia 22904, USA*
[3]*Department of Electrical and Computer Engineering, University of New Mexico, Albuquerque, New Mexico 87106, USA*

(Received 15 February 2011; accepted 30 March 2011; published online 22 April 2011)

We report on the thermal boundary conductance across structurally-variant GaSb/GaAs interfaces characterized by different dislocations densities, as well as variably-rough Al/GaSb interfaces. The GaSb/GaAs structures are epitaxially grown using both interfacial misfit (IMF) and non-IMF techniques. We measure the thermal boundary conductance from 100 to 450 K with time-domain thermoreflectance. The thermal boundary conductance across the GaSb/GaAs interfaces decreases with increasing strain dislocation density. We develop a model for interfacial transport at structurally-variant interfaces in which phonon propagation and scattering parallels photon attenuation. We find that this model describes the measured thermal boundary conductances well.
 [doi:10.1063/1.3581041]

Thermal transport across solid interfaces, which is a major inhibitor of heat flow in nanosystems,[1] is quantified by the thermal boundary conductance, h_K. This quantity is the proportionality constant that relates the heat flux across an interface, q_{int}, to the temperature drop associated with the interfacial region, ΔT, i.e., $h_K = q_{int}/\Delta T$. Although a tremendous amount of work has focused on measurements and theory of thermal transmission across solid interfaces assuming a perfectly abrupt or "flat" junction between two materials (see Refs. 1 and 2 for extensive reviews), measurements of thermal transport across nonideal interfaces are much less frequently studied. Recently, Hopkins *et al.*[3] found that RMS roughness at Al/Si interfaces and elemental mixing at Cr/Si interfaces[4,5] causes variations in h_K at room temperature. Collins and Chen[6] found that the surface chemistry at diamond surfaces can affect h_K across Al/diamond interfaces over a wide temperature range. Understanding the role of imperfect structure at solid interfaces and its role in h_K is of utmost importance to further engineer thermal conduction in nanostructures.

In this work, we measure h_K across GaSb/GaAs interfaces with time-domain thermoreflectance (TDTR). We grow GaSb films on GaAs substrates via two different epitaxial techniques leading to different dislocation densities around the GaSb/GaAs boundary. In addition, these different growth techniques cause the dislocation densities of the GaSb films to vary, thus changing the surface morphology of the films. Therefore, we also study the effect of dislocation density and interface roughness on h_K at Al/GaSb interfaces, as a thin 100 nm Al film is deposited on the GaSb surface for TDTR measurements. We quantify the phonon scattering with a variation in the diffuse mismatch model (DMM) (Ref. 7) in which phonon propagation and scattering parallels photon attenuation. These thermal results have implications for the design, growth, and selection of materials in laser diodes and other gallium-based optoelectronics.

We grow 500 nm of GaSb on GaAs substrates using solid-source molecular beam epitaxy. The lattice mismatch between the two Ga-based binaries is 7.78%. This highly mismatched system reaches its critical thickness within the first monolayer and has the tendency to form islands with interfacial arrays of 90° lomer misfit dislocations.[8] The islands coalesce with further growth and eventually tend to become a planar surface. However, the process of coalescence leads to 60° misfit dislocations that can very easily turn into threading dislocations.[9] We grow one GaSb film via the interfacial-misfit array (IMF) growth mode, a particular growth mode that allows us to achieve large scale IMF dislocation array networks through the use of Sb-rich surface reconstructions resulting in GaSb grown on GaAs with significantly reduced threading dislocations.[10] The threading dislocations for a non-IMF growth of GaSb on GaAs is typically 10^9–10^{11} dislocations per square centimeter, while in the case of the IMF growth mode the threading dislocation density ranges between 5×10^6–5×10^8 dislocations per cm^2. The threading dislocations were measured using plan-view and cross-section transmission electron microscopy.[11,12] Along with the threading dislocations in the material, we also observe that the screw type dislocations are significantly reduced in the IMF sample compared to non-IMF samples. Figure 1 shows atomic force microscopy (AFM) images of the GaSb film surface for the non-IMF [(a) and (b)] and IMF [(c) and (d)] samples. The effect of the high density of screw dislocations is apparent on the surface of the non-IMF sample [Fig. 1(b)]. The rms roughnesses on the GaSb surfaces are 1.7 nm and 2.3 nm for the IMF and non-IMF growth techniques, respectively.

We measure h_K at the Al/GaSb and GaSb/GaAs interfaces with TDTR; typical experimental descriptions of TDTR and details of the thermal and lock-in analyses for thin-film systems are described elsewhere.[13–15] We collect

[a)]Electronic mail: pehopki@sandia.gov.

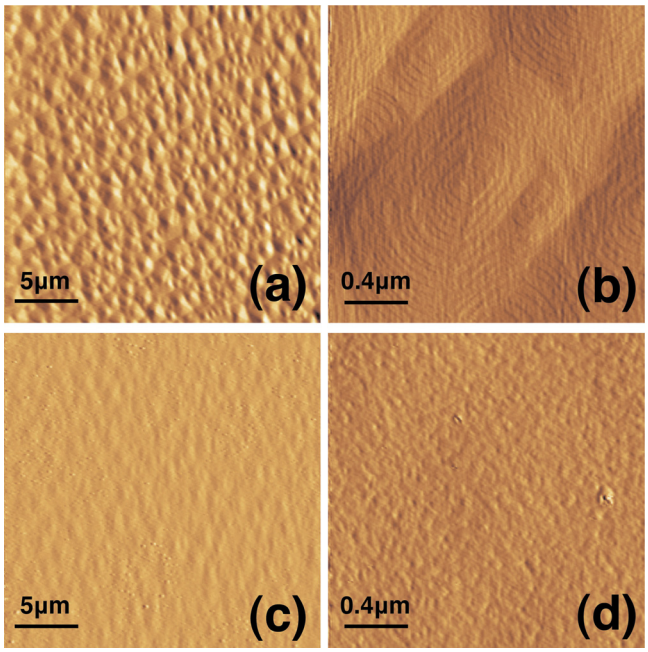

FIG. 1. (Color online) AFM images of the GaSb film surface for the non-IMF [(a) and (b)] and IMF [(c) and (d)] samples.

TDTR data using pump modulation frequencies of 11 and 1.07 MHz. Since the penetration depth of the modulated pump excitation is inversely proportional to the square root of the modulation frequency, the TDTR data taken at 11 MHz has minimal sensitivity to the buried GaSb/GaAs interface compared to 1.07 MHz data. Therefore, we use the two TDTR data sets (11 and 1.07 MHz) to determine h_K at both the Al/GaSb and GaSb/GaAs interfaces in a similar procedure as outlined by Shukla *et al.*[16] In our analysis, we use bulk literature values for the heat capacities of each layer and assume a bulk thermal conductivity of the GaAs substrate.[17–19] We estimate the reduced thermal conductivity of the Al transducer layer from electrical resistivity measurements on the Al film. We slightly adjust the thermal conductivity of the GaSb from that of bulk to improve the quality of the fits to the TDTR data and find that the resultant thermal conductivity is well described by bulk values.[19] Although we expect the thermal conductivity of the GaSb film to be lower than bulk due to film size effects and structural changes from the different growth techniques, the low thermal conductances at the Al/GaSb and GaSb/GaAs interfaces cause the thermal response of our samples to be dominated by the interfaces, and therefore, less sensitive to the reduction in the GaSb thermal conductivity. We verify the 100 nm Al film thickness with picosecond ultrasonics.[20,21]

The measured thermal boundary conductance of the Al/GaSb and GaSb/GaAs interfaces are shown in Fig. 2. The roughnesses of at the GaSb surface, δ, measured via AFM (Fig. 1) are indicated in the figure. For the GaSb/GaAs interfaces, we estimate the spatial extent of the dislocation-dense region as δ, which is valid due to the epitaxial growth conditions as verified by TEM.[11] The roughness induced by the non-IMF growth technique causes approximately a factor of 2 reduction in h_K. Also, the values of h_K at these GaSb-based interfaces are relatively low compared to other solid interfaces.[2,25] The conductances across the GaSb interfaces offer a similar thermal resistances as 50–150 nm of SiO_2. Also plotted in Fig. 2 are the measured values for h_K at

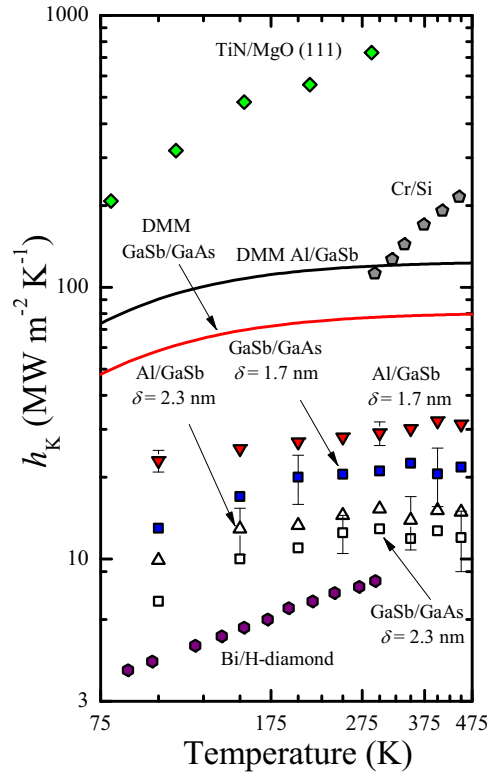

FIG. 2. (Color online) Thermal boundary conductances at the two different Al/GaSb and GaSb/GaAs interfaces studied in this work along with previously measured data at TiN/MgO(111),[22] Cr/Si,[23] and Bi/H-diamond (Ref. 24) interfaces. DMM calculations are shown for the Al/GaSb and GaSb/GaAs interfaces, which drastically overpredict the measured data since the traditional formulation of the DMM does not account for dislocations or roughness around interfaces.

TiN/MgO(111),[22] Cr/Si,[23] and Bi/H-diamond[24] interfaces. The TiN/MgO(111) and Cr/Si interfaces represent relatively "acoustically matched" interfaces (i.e., similar ranges of phonon frequencies, as evaluated by the ratio of materials' Debye temperatures).[26] Al/GaSb and GaSb/GaAs are as acoustically matched as TiN/MgO(111) and Cr/Si, but exhibit drastically different temperature trends and are about an order of magnitude less in value. The values of h_K at the Al/GaSb and GaSb/GaAs interfaces are closer to h_K at Bi/H-diamond interfaces, which are drastically acoustically mismatched materials.

We model h_K at Al/GaSb and GaSb/GaAs interfaces with the DMM.[7] For these calculations, we use the approach that we outlined previously in which we fit a polynomial to a measured or simulated phonon dispersion in one crystallographic direction and assume an isotropic medium to calculate the DMM.[27] For DMM calculations, we use the dispersion in the Γ to X direction of the Brillouin zone from Ref. 28 for Al, Ref. 29 for GaSb, and Ref. 30 for GaAs (we include the optical branches of GaSb and GaAs in our calculations).[31] Calculations of the DMM for the Al/GaSb and GaSb/GaAs interfaces are shown in Fig. 2 (details of our specific DMM calculations and analyses of the assumptions can be found in Refs. 27 and 32). Clearly, the DMM greatly over-predicts the measured values. As the DMM assumes a perfect interface and a single phonon scattering event, this approach is not valid for the dislocation-dense and roughened interfaces studied in this work. To account for the various scattering events at these interfaces, we introduce an

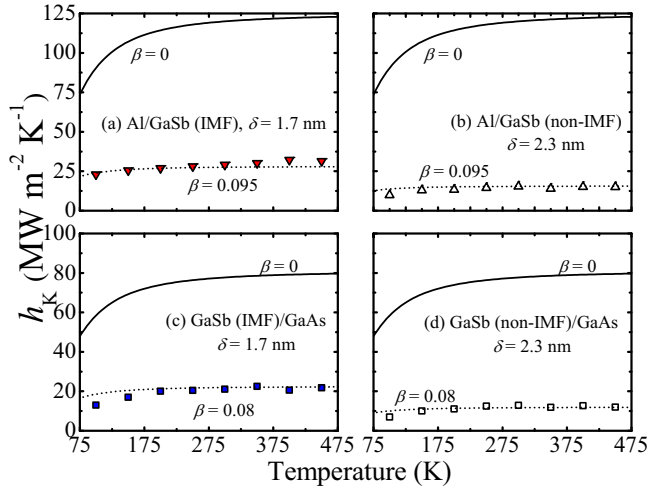

FIG. 3. (Color online) Measured thermal boundary conductances of the Al/GaSb and GaSb/GaAs interfaces along with predictions of the traditional DMM (β=0) and the DMM accounting for additional phonon attenuation around the interface.

"attenuation-type" model, similar to the Beer–Lambert law of photon attenuation, that we have discussed previously.[33] In this approach, the DMM is piecewise defined so that phonons with wavelengths longer than the characteristic length of the structurally variant region, δ, are not affected by the rough region, and therefore their interfacial conductance is governed by that predicted by the DMM. On the other hand, the degree to which phonons with wavelengths shorter than δ are attenuated by this region depends on the relative values of the phonon wavelength, λ, compared to δ, and the phonons propagating in this region are attenuated by a factor $\gamma=\exp[-(4\pi\beta/\lambda)\delta]$. Note that the term $4\pi\beta/\lambda$ exactly parallels the linear attenuation coefficient of photons such that γ is the phonon equivalent of the Beer–Lambert law. For a perfect interface, β, the phonon equivalent of an average, spectrally independent extinction coefficient, goes to zero. Note γ is included in the integrand of the DMM when $\lambda < \delta$. Taking δ as the measured rms roughness of the GaSb surface, the same value for β improves the values and temperature trends at similar interfaces as compared to the DMM (i.e., β=0) regardless of the roughness as seen in Fig. 3. In addition, similar values for β are found for both of the Al/GaSb and GaSb/GaAs interfaces, respectively. This suggests that the dislocations produced by the GaSb film growth modes scatter phonons via the same mechanisms and the decrease in h_K is only due to a greater spatial extent of these phonon scattering mechanisms. This also alludes to the fact that phonon scattering events around interfaces are intrinsic to the materials comprising the interfaces. The slightly higher value for β at the Al/GaSb interface compared to the GaSb/GaAs interface could be due to a thin alloyed region forming of the Al and GaSb which would offer additional scattering mechanisms beyond phonon-dislocation scattering.

In summary, we have measured h_K at structurally variant Al/GaSb and GaSb/GaAs interfaces, finding that h_K across the Al/GaSb and GaSb/GaAs interfaces decrease by increasing strain dislocation density during GaSb film growth.

P.E.H. is appreciative for funding from the LDRD program office through the Sandia National Laboratories Harry S. Truman Fellowship Program. J.C.D. is appreciative for funding from the National Science Foundation Graduate Research Fellowship Program and the Student Intern Program at Sandia National Laboratories. Sandia is a multiprogram laboratory operated by Sandia Corporation, a wholly owned subsidiary of Lockheed Martin Corporation, for the United States Department of Energy's National Nuclear Security Administration under Contract No. DE-AC04-94AL85000.

[1]D. G. Cahill, W. K. Ford, K. E. Goodson, G. D. Mahan, A. Majumdar, H. J. Maris, R. Merlin, and S. R. Phillpot, J. Appl. Phys. **93**, 793 (2003).
[2]E. Pop, Nano Res. **3**, 147 (2010).
[3]P. E. Hopkins, L. M. Phinney, J. R. Serrano, and T. E. Beechem, Phys. Rev. B **82**, 085307 (2010).
[4]P. E. Hopkins and P. M. Norris, Appl. Phys. Lett. **89**, 131909 (2006).
[5]P. E. Hopkins, P. M. Norris, R. J. Stevens, T. Beechem, and S. Graham, J. Heat Transfer **130**, 062402 (2008).
[6]K. C. Collins and G. Chen, Appl. Phys. Lett. **97**, 083102 (2010).
[7]E. T. Swartz and R. O. Pohl, Rev. Mod. Phys. **61**, 605 (1989).
[8]A. M. Rocher, Solid State Phenom. **19–20**, 563 (1991).
[9]W. Qian, M. Skowronski, and R. Kaspi, J. Electrochem. Soc. **144**, 1430 (1997).
[10]S. H. Huang, G. Balakrishnan, A. Khoshakhlagh, A. Jallipalli, L. R. Dawson, and D. L. Huffaker, Appl. Phys. Lett. **88**, 131911 (2006).
[11]A. Jallipalli, G. Balakrishnan, S. H. Huang, T. J. Rotter, K. Nunna, B. L. Liang, L. R. Dawson, and D. L. Huffaker, Nanoscale Res. Lett. **4**, 1458 (2009).
[12]S. Huang, G. Balakrishnan, and D. L. Huffaker, J. Appl. Phys. **105**, 103104 (2009).
[13]P. E. Hopkins, J. R. Serrano, L. M. Phinney, S. P. Kearney, T. W. Grasser, and C. T. Harris, J. Heat Transfer **132**, 081302 (2010).
[14]D. G. Cahill, Rev. Sci. Instrum. **75**, 5119 (2004).
[15]A. J. Schmidt, X. Chen, and G. Chen, Rev. Sci. Instrum. **79**, 114902 (2008).
[16]N. C. Shukla, H. H. Liao, J. T. Abiade, F. Liu, P. K. Liaw, and S. T. Huxtable, Appl. Phys. Lett. **94**, 081912 (2009).
[17]C. Y. Ho, R. W. Powell, and P. E. Liley, J. Phys. Chem. Ref. Data **1**, 279 (1972).
[18]Y. S. Touloukian, R. W. Powell, C. Y. Ho, and P. G. Klemens, *Specific Heat: Nonmetallic Solids* (IFI/Plenum, New York, 1970), Vol. 5.
[19]Y. S. Touloukian, R. W. Powell, C. Y. Ho, and P. G. Klemens, *Thermal Conductivity: Nonmetallic Solids* (IFI/Plenum, New York, 1970), Vol. 2.
[20]C. Thomsen, H. T. Grahn, H. J. Maris, and J. Tauc, Phys. Rev. B **34**, 4129 (1986).
[21]C. Thomsen, J. Strait, Z. Vardeny, H. J. Maris, J. Tauc, and J. J. Hauser, Phys. Rev. Lett. **53**, 989 (1984).
[22]R. M. Costescu, M. A. Wall, and D. G. Cahill, Phys. Rev. B **67**, 054302 (2003).
[23]P. E. Hopkins, R. J. Stevens, and P. M. Norris, J. Heat Transfer **130**, 022401 (2008).
[24]H. K. Lyeo and D. G. Cahill, Phys. Rev. B **73**, 144301 (2006).
[25]R. J. Stevens, A. N. Smith, and P. M. Norris, J. Heat Transfer **127**, 315 (2005).
[26]C. Kittel, *Introduction to Solid State Physics*, 7th ed. (Wiley, New York, 1996).
[27]J. C. Duda, T. Beechem, J. L. Smoyer, P. M. Norris, and P. E. Hopkins, J. Appl. Phys. **108**, 073515 (2010).
[28]G. Gilat and R. M. Nicklow, Phys. Rev. **143**, 487 (1966).
[29]M. K. Farr, J. G. Traylor, and S. K. Sinha, Phys. Rev. B **11**, 1587 (1975).
[30]K. Kunc and R. M. Martin, Phys. Rev. Lett. **48**, 406 (1982).
[31]T. Beechem, J. C. Duda, P. E. Hopkins, and P. M. Norris, Appl. Phys. Lett. **97**, 061907 (2010).
[32]J. C. Duda, P. E. Hopkins, J. L. Smoyer, M. L. Bauer, T. S. English, C. B. Saltonstall, and P. M. Norris, Nanoscale Microscale Thermophys. Eng. **14**, 21 (2010).
[33]P. E. Hopkins, J. C. Duda, C. W. Petz, and J. A. Floro, "Controlling thermal conductance through quantum dot roughening at interfaces," Phys. Rev. B (to be published).